Absence of Dap12 and the αvβ3 integrin causes severe osteopetrosis

Wei Zou[1] and Steven L. Teitelbaum[1,2]

[1]Department of Pathology and Immunology, and [2]Division of Bone and Mineral Diseases, Department of Medicine, Washington University School of Medicine, St. Louis, MO 63110

In vitro, ligand occupancy of αvβ3 integrin induces phosphorylation of Dap12, which is essential for osteoclast function. Like mice deleted of only αvβ3, Dap12$^{-/-}$ mice exhibited a slight increase in bone mass, but Dap12$^{-/-}$ mice, lacking another ITAM protein, FcRγ, were severely osteopetrotic. The mechanism by which FcRγ compensates for Dap12 deficiency is unknown. We find that co-deletion of FcRγ did not exacerbate the skeletal phenotype of β3$^{-/-}$ mice. In contrast, β3/Dap12 double-deficient (DAP/β3$^{-/-}$) mice (but not β1/Dap12 double-deficient mice) were profoundly osteopetrotic, reflecting severe osteoclast dysfunction relative to those lacking αvβ3 or Dap12 alone. Activation of OSCAR, the FcRγ co-receptor, rescued Dap12$^{-/-}$ but not DAP/β3$^{-/-}$osteoclasts. Thus, the absence of αvβ3 precluded compensation for Dap12 deficiency by FcRγ. In keeping with this, Syk phosphorylation did not occur in OSCAR-activated DAP/β3$^{-/-}$ osteoclasts. Thus, FcRγ requires the osteoclast αvβ3 integrin to normalize the Dap12-deficient skeleton.

Introduction

The osteoclast is the principal skeletal resorptive cell with the capacity to degrade the organic and inorganic matrices of bone (Novack and Teitelbaum, 2008). It exerts its bone-degrading properties by attaching to mineralized matrix and forming actin rings that isolate the resorptive microenvironment from the general extracellular space. Skeletal degradation, by the osteoclast, is initiated by transport of H^+ and Cl^- ions into the resorptive space juxtaposed to bone. The consequential acidification mobilizes the mineral phase of bone, thereby exposing its organic matrix, which is degraded by exocytically transported cathepsin K. Resorption, therefore, requires delivery of bone-degrading molecules to the bone/cell interface involving polarization of the osteoclast via organization of its actin cytoskeleton.

Immunoreceptor tyrosine–based activation motif (ITAM)–containing co-activators, which participate in innate immunity, are also central to osteoclastic bone resorption (Humphrey et al., 2005). Because their extracellular domains are small and therefore incapable of recognizing ligand, ITAM proteins associate via their transmembrane regions, with plasmalemma-residing immunoreceptors. In consequence, a host of signaling cascades regulating proliferation, survival, and cytoskeletal organization are activated.

To date, two ITAM co-activating adaptor proteins, Dap12 and FcRγ, are established as functional in osteoclasts. Dap12 associates with its co-receptors, TREM2 and SIRPβ1, in these cells, whereas FcRγ recognizes OSCAR and PIR-A (Koga et al., 2004; Mócsai et al., 2004). Deletion of FcRγ has no effect on the osteoclast, in vitro or in vivo, and knockout animals exhibit no skeletal abnormalities. Dap12-deficient BM macrophages (BMMs) also normally express markers of osteoclast differentiation when exposed to macrophage colony-stimulating factor (M-CSF) and receptor activator of nuclear factor κB ligand (RANKL), but unlike those lacking FcRγ, fail to optimally organize their cytoskeleton or resorb bone in vitro (Mócsai et al., 2004; Zou et al., 2010). This resorptive dysfunction reflects absence of the essential role of Dap12 in recruiting Syk to the αvβ3-initiated signaling complex (Zou et al., 2008).

Not surprisingly, in face of the purported linear inclusion of αvβ3 and Dap12 in the same signaling complex, cultured osteoclasts, lacking either protein, have similar façades. In contrast to their abnormal in vitro phenotype, however, Dap12$^{-/-}$ mice contain normal appearing osteoclasts and, again, like those deficient in αvβ3, exhibit only a modest increase in bone mass. The preponderance of evidence indicates the paradox of a robust

Correspondence to Steven L. Teitelbaum: teitelbs@wustl.edu

Abbreviations used in this paper: Ab, antibody; BMM, BM macrophage; ITAM, immunoreceptor tyrosine–based activation motif; M-CSF, macrophage colony-stimulating factor; RANKL, receptor activator of nuclear factor κB ligand.

The Rockefeller University Press $30.00
J. Cell Biol. Vol. 208 No. 1 125–136
www.jcb.org/cgi/doi/10.1083/jcb.201410123

in vitro osteoclast phenotype and a virtually normal Dap12$^{-/-}$ skeleton, reflecting in vivo compensation by FcRγ (Koga et al., 2004; Mócsai et al., 2004). This posture is underscored by the severe osteopetrosis of mice lacking Dap12 and FcRγ, in combination, despite the absence of a significant skeletal phenotype when either is deleted alone. The mechanism by which FcRγ compensates for lack of Dap12 in promoting osteoclast function is unknown.

Because β3 and Dap12 are believed to be linear components of the same cytoskeleton-organizing signaling complex (Zou et al., 2007), we posited that combined deficiency of the two would mirror the mild skeletal phenotype characterizing single gene deletion of either. To our surprise, mice lacking both genes (DAP/β3$^{-/-}$) exhibit severe osteopetrosis with a 400% increase in trabecular bone mass. In contrast, co-deletion of FcRγ and β3 does not alter the β3$^{-/-}$phenotype. In keeping with the severity of their osteopetrosis, the osteoclasts of DAP/β3$^{-/-}$mice effectively differentiate but appear strikingly abnormal, in vitro and in vivo. In contrast co-deletion of Dap12 and the β1 integrin (DAP/β1$^{-/-}$) subunit yields mice with normal skeletal mass and osteoclasts indistinguishable from those lacking only Dap12. The unexpected phenotype of DAP/β3$^{-/-}$ mice and its distinction from DAP/β1$^{-/-}$, establish that the ability of FcRγ to compensate for Dap12 deletion, in osteoclasts, specifically requires αvβ3. As such, activation of FcRγ's co-receptor, OSCAR, substantially rescues Dap12$^{-/-}$ osteoclasts only in the presence of the integrin. Furthermore, absence of Dap12 and αvβ3 obviates compensation by other integrins. It also reduces phosphorylation of Syk, a tyrosine kinase essential to osteoclast cytoskeleton organization. These studies provide a mechanistic basis for the enigmatic role of FcRγ in enabling Dap12-deficient osteoclastic bone resorption. They also establish that αvβ3 mediates the compensatory properties of ITAM co-stimulatory proteins in osteoclasts.

Results

DAP/β3$^{-/-}$ mice are osteopetrotic

DAP/β3$^{-/-}$ mice are born in Mendelian frequency and like those lacking only β3 are predisposed to hemorrhage (McHugh et al., 2000). Interestingly, DAP/β3$^{-/-}$ mice are approximately half the size of those deleted of only one of the two genes that are indistinguishable from WT (Fig. 1, A and B). Radiographical and μCT analysis of the distal femurs of β3$^{-/-}$ and Dap12$^{-/-}$ 4-wk-old mice mirror that of WT (Fig. 1, C and D). In contrast, trabecular bone of DAP/β3$^{-/-}$ mice is increased by >400%, and the long bones are radiodense. These radiographical and μCT features are confirmed by histomorphometry (Fig. 1, E and F). DAP/β3$^{-/-}$ bone also contains cartilaginous bars deep within the metaphysis, a characteristic feature of osteopetrosis, a family of disorders of increased skeletal mass due to arrested resorption (Tolar et al., 2004). Also in keeping with attenuated resorption, modeling of DAP/β3$^{-/-}$ bones is abnormal as evidenced by broadening of the distal femoral diaphysis and metaphysis (Fig. 1 G).

DAP/β3$^{-/-}$ osteoclast cytoskeleton is disorganized

Dap12$^{-/-}$ and β3$^{-/-}$ BMMs, exposed to RANKL and M-CSF, differentiate into cells that are universally TRAP expressing (Fig. 2 A). Although many multinucleate, they fail to optimally spread. RANKL/M-CSF–treated BMMs lacking both Dap12 and β3 also universally express TRAP. However, the abnormal features of DAP/β3$^{-/-}$ osteoclasts are more striking than those lacking only one gene, as there is no evidence of multinucleation. The double-deleted cells also have a crenated facade, indicating severe cytoskeletal abnormalities. Although the TRAP-stained Dap12$^{-/-}$ and β3$^{-/-}$ osteoclasts appear to be virtually identical, the integrin-deleted cells generate actin rings, which is abnormal; these structures are small and rare in those lacking Dap12 (Faccio et al., 2003a; Zou et al., 2008; Fig. 2 B). Consistent with their more abnormal phenotype, DAP/β3$^{-/-}$ osteoclasts are incapable of producing actin rings. Transduction of DAP/β3$^{-/-}$ BMMs with either Dap12 or β3 yields the TRAP-stained phenotype of single gene-deleted osteoclasts (Fig. 2 C). Co-transduction with both, however, completely normalizes the double-deleted cells.

In contrast to their severe morphological abnormalities, temporal expression of osteoclast differentiation markers by DAP/β3$^{-/-}$ BMMs is indistinguishable from those lacking Dap12, which we have established are unimpaired (Fig. 2 D) (Zou et al., 2008). Consistent with intact differentiation in vitro, DAP/β3$^{-/-}$ mice contain normal numbers of osteoclasts (Fig. 2 E). DAP/β3$^{-/-}$ osteoclasts, however, have the irregular appearance of those with dysfunctional cytoskeletons, are reduced in size, and attach poorly to bone (Fig. 2, F–H), thus yielding decreased eroded trabecular surface (Fig. 2 I). Whereas serum CTx, a clinical marker of bone resorption, is unaltered in β3$^{-/-}$ and Dap12$^{-/-}$ mice, it is reduced by ∼50% in those lacking both genes, confirming impaired osteoclast activity (Fig. 2 J).

These data confirm attenuated bone resorption in DAP/β3$^{-/-}$ mice. To determine if this abnormality is endogenous in the osteoclast or the product of osteoclast-modifying cells, such as osteoblasts, we determined the osteoclastogenic capacity of various co-cultures of WT and DAP/β3$^{-/-}$ BMMs and osteoblasts. As illustrated in Fig. 2 K, a combination of DAP/β3$^{-/-}$ BMMs and WT osteoblasts yields osteoclasts indistinguishable from those derived from pure populations of double-deleted progenitors. In contrast, osteoclasts generated in co-cultures of WT BMMs and DAP/β3$^{-/-}$ osteoblasts appear to be normal. Thus, the abnormal phenotype of DAP/β3$^{-/-}$ osteoclasts reflects a cell autonomous mechanism.

Bone remodeling is characterized by coupling of bone resorption and formation. Thus, a reasonable hypothesis holds that the arrested osteoclastic activity extant in DAP/β3$^{-/-}$ mice would be attended by suppressed osteogenesis. In fact, osteoblast abundance and circulating osteocalcin, a specific marker of bone formation, are reduced in the mutant animals (Fig. 2 L). As arrested bone formation would negatively impact bone mass, this observation indicates that the magnitude of osteoclast dysfunction is greater than reflected in the 400% increase in DAP/β3$^{-/-}$ trabecular bone volume.

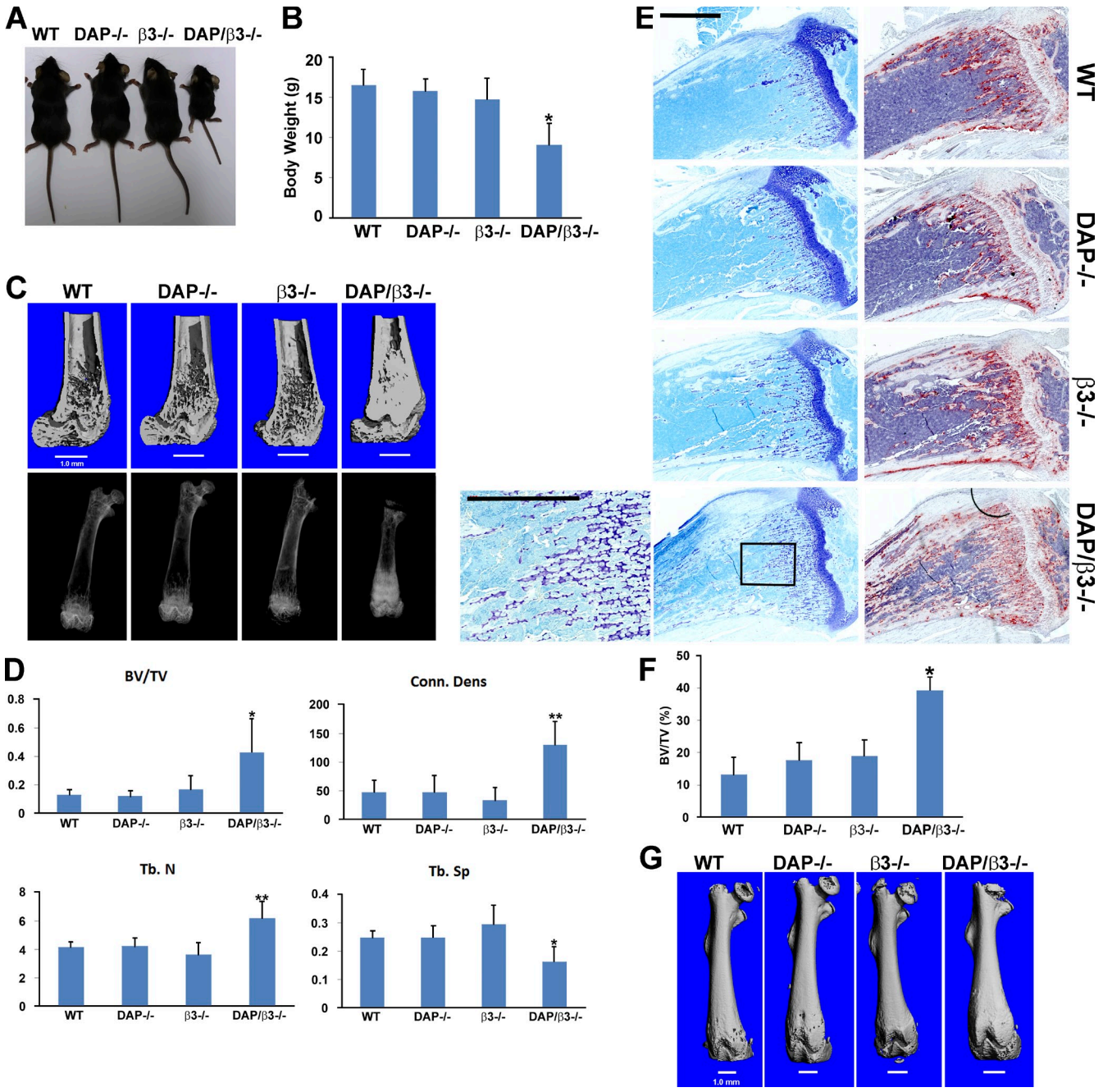

Figure 1. **DAP/β3$^{-/-}$ mice are osteopetrotic.** (A) Photograph illustrating runting of 4-wk-old DAP/β3$^{-/-}$ mice. (B) Weight of 4-wk-old WT, Dap12$^{-/-}$, β3$^{-/-}$, and DAP/β3$^{-/-}$ mice. (C) μCT (top) and radiographical (bottom) images of femurs of 4-wk-old WT, Dap12$^{-/-}$, β3$^{-/-}$, and DAP/β3$^{-/-}$ mice. (D) μCT-determined trabecular bone parameters of 4-wk-old WT, Dap12$^{-/-}$, β3$^{-/-}$, and DAP/β3$^{-/-}$ mice. (E) Histological sections of tibia of 4-wk-old WT, Dap12$^{-/-}$, β3$^{-/-}$, and DAP/β3$^{-/-}$ mice stained (right) for TRAP activity to visualize osteoclasts (red reaction product) or (left) with toluidine blue to visualize cartilage (bottom left). High magnification of delineated area illustrates cartilaginous bars (purple reaction product) diagnostic of severe osteopetrosis. Bars, 500 μm. (F) Histomorphometric analysis of BV/TV of 4-wk-old WT, Dap12$^{-/-}$, β3$^{-/-}$, and DAP/β3$^{-/-}$ mouse tibia. (G) μCT image of 4-wk-old WT, Dap12$^{-/-}$, β3$^{-/-}$, and DAP/β3$^{-/-}$ mice documenting bone modeling defect in the latter. *, P < 0.05; **, P < 0.01.

The osteopetrosis of ITAM protein-deficient, β3$^{-/-}$ mice, is Dap12-specific

The negative effect of conjoint Dap12 deletion on β3$^{-/-}$ osteoclasts raised the question as to whether absence of the other osteoclast-expressed ITAM protein, FcRγ, also impacts these β3-deficient cells. To address this issue, we crossed FcRγ$^{-/-}$ and β3$^{-/-}$ mice (FcRγ/β3$^{-/-}$). Deletion of the two genes yields osteoclasts identical to those lacking only the integrin, both in appearance and bone resorptive capacity (Fig. 3, A and B). Consistent with these in vitro observations, trabecular bone volume of FcRγ/β3$^{-/-}$ mice is indistinguishable from that of FcRγ$^{-/-}$ (Fig. 3 C). Thus, unlike the synergistic effect of Dap12 deletion on the phenotype of β3$^{-/-}$ osteoclasts, additional absence of FcRγ is inconsequential.

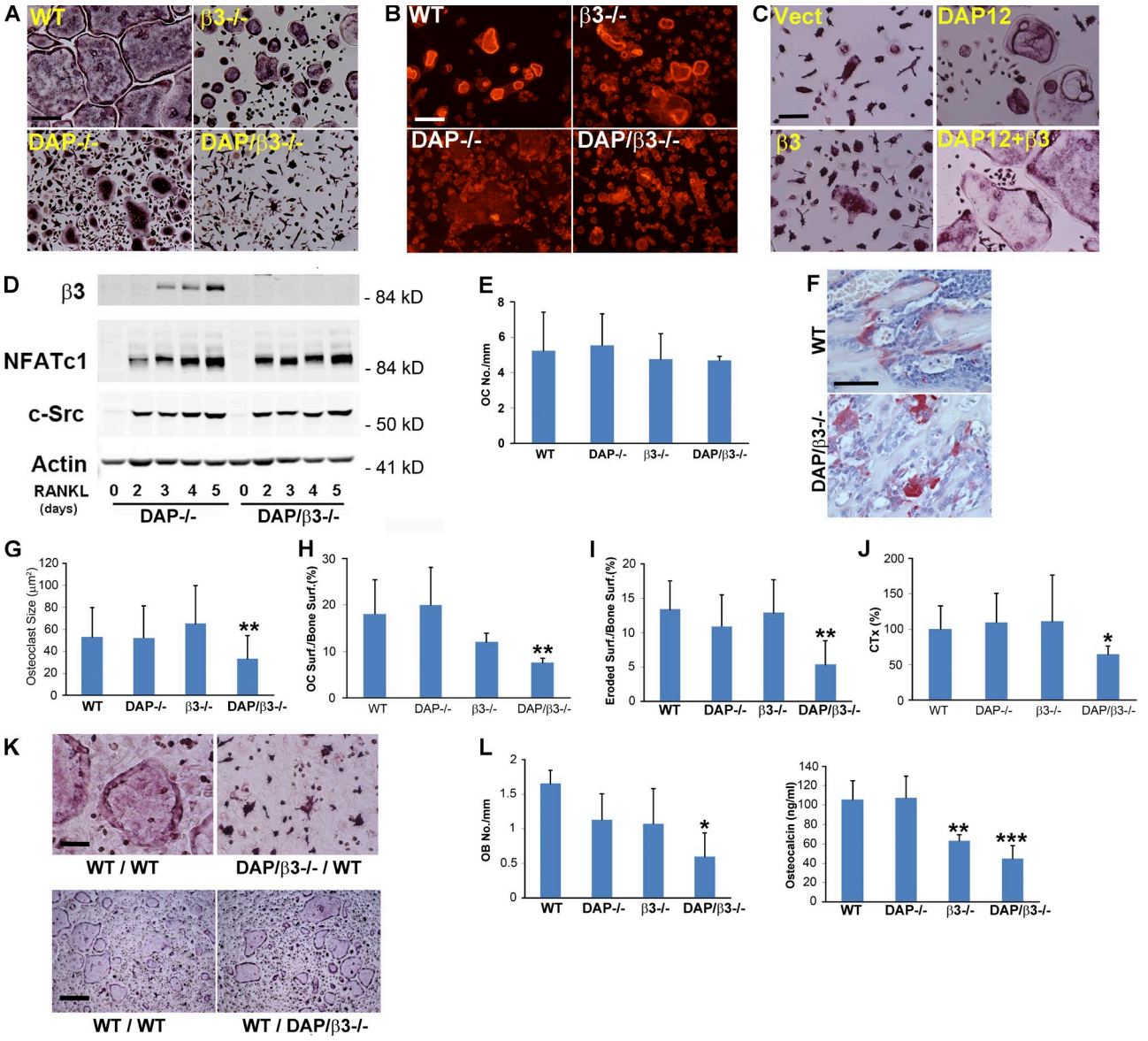

Figure 2. **DAP/β3$^{-/-}$ osteoclast cytoskeleton is disorganized.** (A) WT, Dap12$^{-/-}$, β3$^{-/-}$, and DAP/β3$^{-/-}$ BMMs, cultured on plastic, were exposed to M-CSF and RANKL. At day 5, the cells were stained for TRAP activity. Bar, 500 µm. (B) WT, Dap12$^{-/-}$, β3$^{-/-}$, and DAP/β3$^{-/-}$ BMMs, cultured on bone, were exposed to M-CSF and RANKL. On day 5, the cells were stained with Alexa Fluor 543-phalloidin to visualize actin rings. Bar, 100 µm. (C) DAP/β3$^{-/-}$ BMMs, transduced with Dap12, WT β3, alone, or in combination, were exposed to M-CSF and RANKL. On day 5, the cells were stained for TRAP activity. Vector transductants served as control. Bar, 100 µm. (D) Dap12$^{-/-}$ and DAP/β3$^{-/-}$ BMMs were treated with M-CSF and RANKL. Osteoclast differentiation proteins were immunoblotted with time. (E) Histomorphometric determination of osteoclast number/mm bone surface in WT, Dap12$^{-/-}$, β3$^{-/-}$, and DAP/β3$^{-/-}$ mice. (F) TRAP-stained histological sections of tibia illustrating attachment of WT (top) osteoclasts to bone and failure of DAP/β3$^{-/-}$ osteoclasts (bottom) to do so. Bar, 50 µm. Histomorphometric quantitation of osteoclast (G) size and (H) number juxtaposed to the bone surface as well as (I) percentage of eroded trabecular surface. (J) Serum CTx of WT, Dap12$^{-/-}$, β3$^{-/-}$ and DAP/β3$^{-/-}$ mice. (K) TRAP stained co-cultures of WT BMMS and WT osteoblasts (top and bottom left, respectively), DAP/β3$^{-/-}$ BMMs and WT osteoblasts (top right), and WT BMMs and DAP/β3$^{-/-}$ osteoblasts (bottom left). Bars: (top) 100 µm; (bottom) 500 µm. (L) Histomorphometric analysis of osteoblast number/mm bone surface (left) and serum osteocalcin (right). *, P < 0.05; **, P < 0.01; ***, P < 0.001.

β3 integrin regulates FcRγ's capacity to rescue Dap12-deficient osteoclasts

These data indicate the compensatory effect of FcRγ on Dap12$^{-/-}$ osteoclasts requires αvβ3. To test this hypothesis, we used FLAG-tagged OSCAR, which activates FcRγ when stimulated by anti-FLAG Ab (Zou et al., 2010). OSCAR-FcRγ activation increases the capacity of Dap12$^{-/-}$ osteoclasts to spread only in the presence of αvβ3 (Fig. 4 A). Moreover, OSCAR-transduced Dap12$^{-/-}$ osteoclasts on bone, which contains the natural OSCAR ligand, form actin rings and resorb bone; no such effect occurs in DAP/β3$^{-/-}$ osteoclasts (Fig. 4, B–D). On the other hand, OSCAR-FLAG, stimulated by FLAG antibody (Ab), converts the appearance of DAP/β3$^{-/-}$ osteoclasts to those exclusively lacking Dap12 only in the presence of the β3 integrin (Fig. S1). Consistent with our previous observation (Zou et al., 2010), OSCAR activation does not regulate

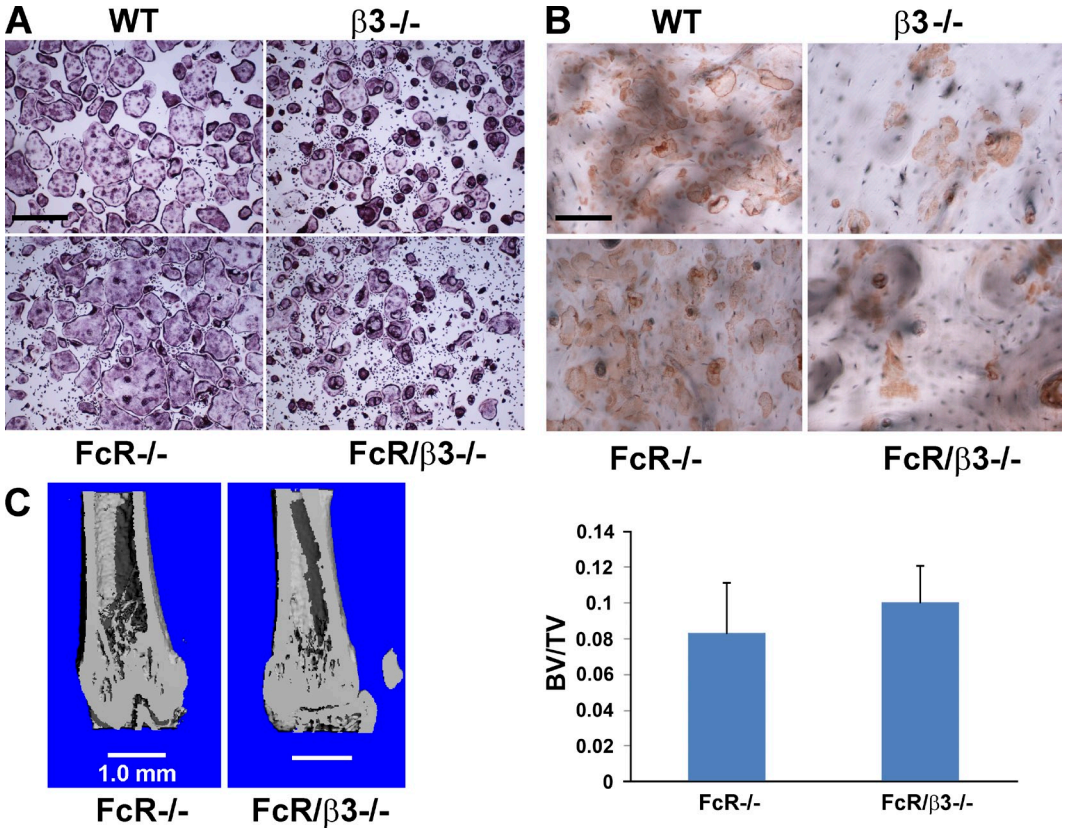

Figure 3. **The osteopetrosis of ITAM protein/β3$^{-/-}$ mice is Dap12 specific.** (A) WT, β3$^{-/-}$, FcRγ$^{-/-}$, and FcRγ/β3$^{-/-}$ BMMs, cultured in the presence of M-CSF and RANKL for 5 d, were stained for TRAP activity. Bar, 500 µm. (B) WT, β3$^{-/-}$, FcRγ$^{-/-}$ and FcRγ/β3$^{-/-}$ BMMs were cultured, on bone, in the presence of M-CSF and RANKL. After 5 d, the cells were removed and resorption pits were visualized by peroxidase-conjugated wheat germ agglutinin/horse radish peroxidase staining. Bar, 100 µm. (C) FcRγ$^{-/-}$ and FcRγ/β3$^{-/-}$ mouse tibia were subjected to µCT analysis (left) and BV/TV was determined (right).

osteoclast proliferation (Fig. 4 E), but inhibits apoptosis of osteoclasts deprived of M-CSF even in the absence of DAP12 and the integrin (Fig. 4 F).

These data indicate that OSCAR/FcRγ and αvβ3 partner to compensate for the cytoskeletal consequences of Dap12 deletion in osteoclasts. If this is the case, one would expect FcRγ and/or its activating co-receptor, OSCAR, to associate with the integrin. To determine if such is the case, we first transfected 293T cells with human β3, FcRγ, and OSCAR-FLAG. Human β3, whose cytoplasmic domain is identical to that of mouse, was used due to availability of an immunoprecipitating mAb. Immunoblotting each of the transduced constructs, in β3 immunoprecipitates establishes that, in the context of overexpression, the three proteins associate (Fig. 5 A).

We next asked if FcRγ/OSCAR association requires the integrin in authentic osteoclasts. In fact, FcRγ and OSCAR co-immunoprecipitate in DAP/β3$^{-/-}$ prefusion osteoclasts as effectively as in WT cells or those lacking Dap12 (Fig. 5 B). Furthermore, the β3 integrin associates with OSCAR and FcRγ in primary osteoclastic cells treated with M-CSF or RANKL, which promote the capacity of the mature polykaryon to organize its cytoskeleton (Zou et al., 2008; Fig. 5 C–E).

Dap12/β3 deletion prevents compensatory integrin activation

In other cells, β1 integrins activate a cytoskeleton-organizing complex similar to that extant in osteoclasts. In fact, β1 integrins recognize Syk in the bone resorptive cells, independent of the presence of β3 (Zou et al., 2007). Additionally, M-CSF activates the β1 integrin subunit in osteoclasts, as evidenced by induced talin binding (Zou et al., 2013). These observations raise the possibility that combined deletion of Dap12 and the β1 integrin may mirror DAP/β3$^{-/-}$ osteoclasts. We therefore mated Dap12$^{-/-}$ mice and those bearing β1 floxed alleles. The product was crossed to mice expressing LysM Cre, yielding animals with myeloid lineage deletion of the β1 integrin and global absence of Dap12 (DAP/β1$^{-/-}$). BMMs obtained from these mice were exposed to RANKL and M-CSF, which generated cells normally expressing osteoclast differentiation markers (Fig. 6 A). DAP/β1$^{-/-}$ cells are indistinguishable from those lacking only Dap12 (Fig. 6 B). Thus, DAP/β1$^{-/-}$ osteoclasts differ from DAP/β3$^{-/-}$, which are more abnormal than those absent only Dap12. This experiment suggests that unlike β3, absence of the β1 integrin does not aggravate the Dap12$^{-/-}$ osteoclast phenotype. This conclusion is supported by the

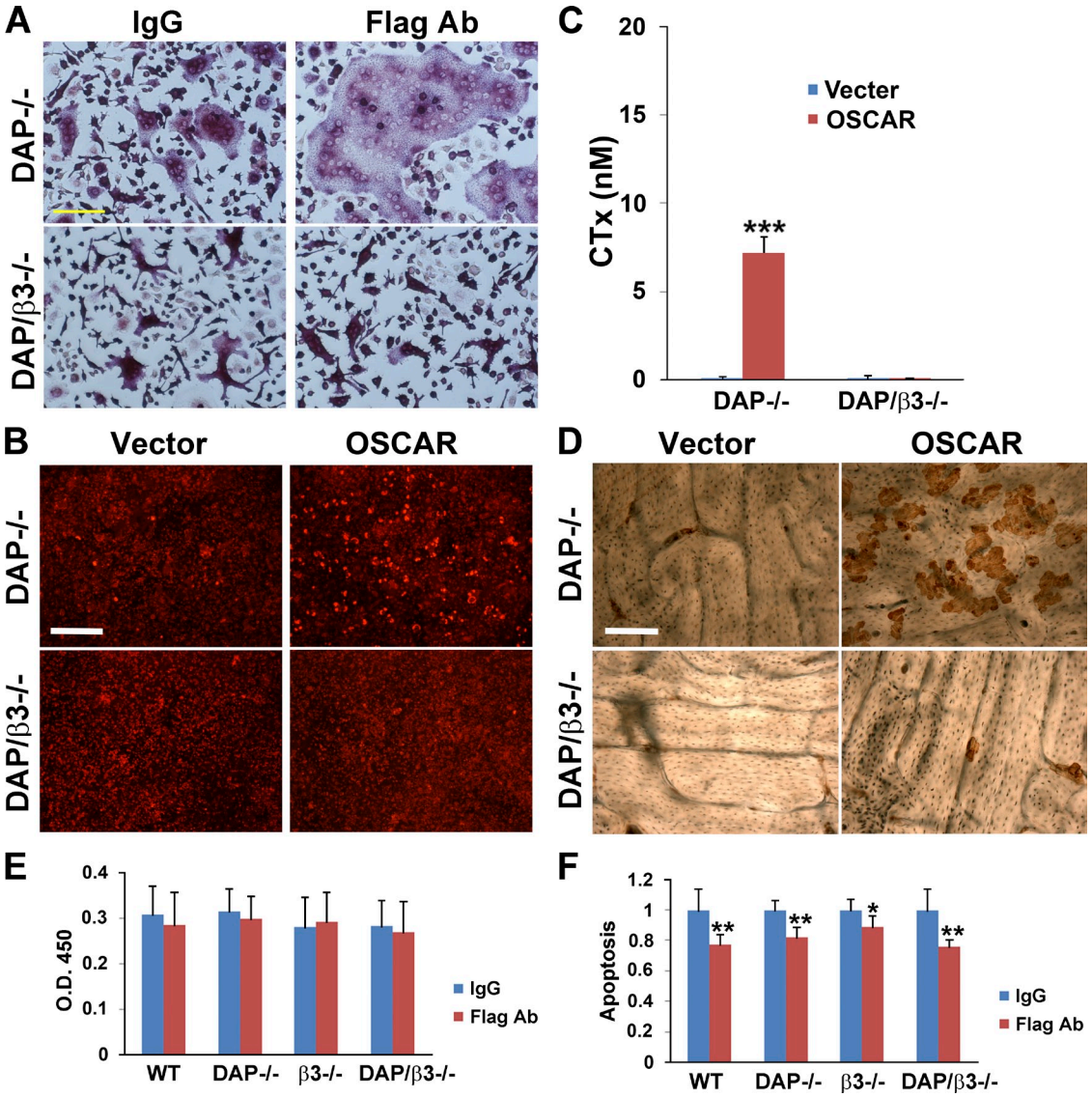

Figure 4. **β3 integrin regulates FcRγ's capacity to rescue DDap12$^{-/-}$ osteoclasts.** (A) OSCAR-FLAG-transduced Dap12$^{-/-}$ or DAP/β3$^{-/-}$ BMMS were plated on IgG- or anti-FLAG Ab–coated plastic. The cells were exposed to RANKL and M-CSF for 5 d and stained for TRAP activity. Bar, 100 µm. (B) OSCAR-FLAG-transduced Dap12$^{-/-}$ or DAP/β3$^{-/-}$ BMMS, were plated on bone. The cells were exposed to RANKL and M-CSF for 5 d and stained with Alexa Fluor 543–phalloidin to visualize actin rings. Bar, 500 µm. (C) Dap12$^{-/-}$ and DAP/β3$^{-/-}$ BMMs, transduced with OSCAR or vector, were cultured on bone in the presence of M-CSF and RANKL. 5 d later, medium CTx content was determined. (D) OSCAR-FLAG–transduced Dap12$^{-/-}$ or DAP/β3$^{-/-}$ BMMS were plated on bone. The cells were exposed to RANKL and M-CSF. After 5 d, the cells were removed and resorption pits were visualized by peroxidase-conjugated wheat germ agglutinin/horse radish peroxidase staining. Bar, 100 µm. (E) M-CSF–induced proliferation of WT and DAP/β3$^{-/-}$ BMMs as a function of BrdU incorporation. (F) Apoptosis of WT and DAP/β3$^{-/-}$ serum and M-CSF–deprived preosteoclasts transfected with OSCAR-FLAG plated on IgG or anti-FLAG mAb. Data are normalized to WT. *, P < 0.05; **, P < 0.01; ***, P < 0.001.

capacity of activated OSCAR to enhance cell spreading, actin ring formation and bone resorptive capacity of DAP/β1$^{-/-}$ osteoclasts as effectively as those lacking only Dap12 (Fig. 6, C–E). Finally, whereas the trabecular bone mass of DAP/β3$^{-/-}$ mice is markedly increased (Fig. 1), DAP/β1$^{-/-}$ mice mirror Dap12$^{-/-}$ (Fig. 6 F).

These studies establish that unlike β3, absence of the β1 integrin does not compromise the Dap12$^{-/-}$ osteoclast phenotype. On the other hand, the β1 integrin subunit probably compensates, in part, for absence of αvβ3 in osteoclasts (Helfrich et al., 1996). For example, osteopetrosis of mice deleted of talin, Rap1 or kindlin 3, which are necessary for global β integrin activation, is substantially more severe than of those lacking αvβ3 (Schmidt et al., 2011; Zou et al., 2013). Furthermore, combined deletion of β3 and other integrin subunits yields a much more abnormal osteoclast phenotype than absence any β integrin, alone (Schmidt et al., 2011).

These observations suggest the robust phenotype of DAP/β3$^{-/-}$ osteoclasts, relative to those lacking only a single gene, may reflect functional deficiency of multiple β integrin subunits. If true, absence of β3 and Dap12 may incapacitate global integrin activators such as talin and thus prevent β1-mediated compensation. We therefore exposed β3$^{-/-}$, Dap12$^{-/-}$, and DAP/β3$^{-/-}$ prefusion osteoclasts to M-CSF, which organizes

the osteoclast cytoskeleton in a talin/β integrin-dependent manner (Zou et al., 2013). Although M-CSF increases β1/talin association in $\beta3^{-/-}$ and $Dap12^{-/-}$ cells, the magnitude of binding is more robust in the absence of β3 than Dap12 (Fig. 6 G). This observation likely reflects lack of competition for talin, by β3, in cells lacking the integrin (Calderwood et al., 2004). In contrast to the robust β1/talin binding in $\beta3^{-/-}$ cells, DAP/$\beta3^{-/-}$ osteoclasts exhibit minimal β1/talin association in the presence or absence of M-CSF. Thus, β1 integrin activation is enhanced in osteoclasts lacking only β3 but compromised by combined absence of the β3 subunit and Dap12. This observation explains the compensatory effect of β1 in $\beta3^{-/-}$ osteoclasts and its inability to modify DAP/$\beta3^{-/-}$ cells.

Syk activation is disrupted in DAP/$\beta3^{-/-}$ osteoclasts

Syk phosphorylation is central to organization of the osteoclast cytoskeleton, whether induced by ligand-mediated (outside-in) or M-CSF–stimulated (inside-out) integrin activation (Zou et al., 2007, 2008). Neither ligand- (Faccio et al., 2003b) nor cytokine-activated (Zou et al., 2008) integrins, however, phosphorylate Syk in $Dap12^{-/-}$ osteoclastic cells maintained on plastic, nor do they normalize their cytoskeleton (Faccio et al., 2003a,b; Zou et al., 2008).

Although M-CSF also fails to phosphorylate Syk in plastic-residing $Dap12^{-/-}$ osteoclasts, it modestly does so when they are cultured on bone (Fig. 7 A). As activated FcRγ is compensatory for absence of Dap12, this observation is consistent with evidence that OSCAR, which activates FcRγ, is a collagen receptor and bone matrix is likely a principal source of OSCAR ligand (Zou et al., 2010; Barrow et al., 2011). Given the central role of Syk in osteoclast function, the profound skeletal phenotype of DAP/$\beta3^{-/-}$ mice may reflect failure of activated FcRγ to induce cytoskeleton-organizing signals without αvβ3.

We find that OSCAR-FLAG–bearing $Dap12^{-/-}$ osteoclasts plated on the αvβ3 ligand vitronectin do not phosphorylate Syk in the absence of FLAG Ab (Fig. 7 B). Conversely, αvβ3 occupancy by vitronectin in the presence of FLAG-Ab–activated OSCAR promotes Syk phosphorylation. Confirming OSCAR-FLAG activates Syk via FcRγ in Dap12-deficient cells, deletion of both ITAM proteins obviates Syk phosphorylation by FLAG Ab (Fig. 7 C). Thus, in $Dap12^{-/-}$ osteoclasts, αvβ3 occupancy and activated FcRγ trigger a key cytoskeleton-organizing complex, in a mutually dependent manner.

These studies involved OSCAR stimulation by anti-FLAG Ab. We next determined the impact of combined Dap12/β3 deletion on FcRγ's capacity to activate Syk in the context of physiological OSCAR ligand. To this end, we generated prefusion OSCAR-transduced osteoclasts on bone. We then exposed the cells to M-CSF which, by stimulating Rap1 and promoting talin association, is a global activator of β integrins (Zou et al., 2013). Thus, M-CSF in collaboration with β integrins, induces Syk-mediated WT osteoclast cytoskeletal organization and bone resorption via inside-out integrin activation. M-CSF promotes Syk phosphorylation in OSCAR-transduced, $Dap12^{-/-}$ cells on bone (Fig. 7 D), which is consistent with the capacity of OSCAR to enhance the resorptive activity of $Dap12^{-/-}$ osteoclasts (Zou et al., 2010). M-CSF, however, fails to stimulate Syk phosphorylation on bone-residing osteoclasts in the combined absence of Dap12 and αvβ3. M-CSF stimulates Syk phosphorylation in OSCAR- but not in vector-transduced $Dap12^{-/-}$ osteoclasts generated on bone (Fig. 7 E), indicating its effect is mediated by OSCAR. In contrast, M-CSF fails to phosphorylate Syk in plastic-residing, OSCAR-transduced $Dap12^{-/-}$ osteoclasts (Fig. 7 F). Thus, regulation of $DAP12^{-/-}$ osteoclast function, by M-CSF requires FcRγ activation. The attenuated Syk activation in DAP/$\beta3^{-/-}$ osteoclasts, even in the presence of activated OSCAR, suggests their severe phenotype reflects inability of FcRγ to induce cytoskeleton-organizing signals without αvβ3. Furthermore, overexpression of WT Syk in DAP/$\beta3^{-/-}$ osteoclasts does not rescue their morphology (Fig. 7 G) or inability to generate actin rings (Fig. 7 H). Hence, regardless of the abundance of the tyrosine kinase, Syk must be activated to organize the osteoclast cytoskeleton, which can be mediated by FcRγ only in the presence of the αvβ3 integrin.

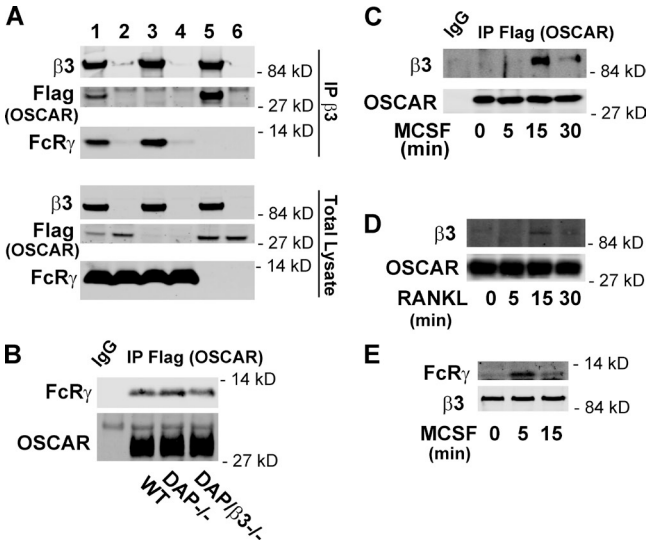

Figure 5. **β3 integrin associates with OSCAR and FcRγ in osteoclasts.** (A) 293T cells were transfected with human β3, FcRγ, and OSCAR-FLAG (lane 1), FcRγ and OSCAR-FLAG (lane 2), β3 and FcRγ (lane 3), FcRγ (lane 4), β3 and OSCAR-FLAG (lane 5), or OSCAR-FLAG (lane 6). β3 immunoprecipitates and total cell lysates were immunoblotted for β3, FcRγ, and FLAG. (B) WT, $Dap12^{-/-}$, and DAP/$\beta3^{-/-}$ BMMS were transduced with OSCAR-FLAG. The cells were exposed to RANKL and M-CSF for 3 d. FLAG immunoprecipitates were immunoblotted for FcRγ and FLAG. Vector-transduced WT cells (first lane) serve as control. (C) WT BMMs, transduced with OSCAR-FLAG were exposed to RANKL and M-CSF for 3 d. After cytokine/serum starvation, the cells were treated with M-CSF. FLAG immunoprecipitates were temporally immunoblotted for β3 and OSCAR. IgG immunoprecipitates serve as control. (D) WT BMMs, transduced with OSCAR-FLAG were exposed to RANKL and M-CSF for 3 d. After cytokine/serum starvation the cells were treated with RANKL and FLAG immunoprecipitates temporally immunoblotted for β3 and OSCAR. (E) $\beta3^{-/-}$ BMMs, transduced with human β3 were exposed to RANKL and M-CSF for 3 d. After cytokine/serum starvation, the cells were treated with M-CSF and β3 immunoprecipitates temporally immunoblotted for β3 and FcRγ.

Discussion

Because resorption requires attachment of osteoclasts to the bone surface, we posited that integrins are central to the process. A series of in vitro experiments indicated αvβ3 is the principal

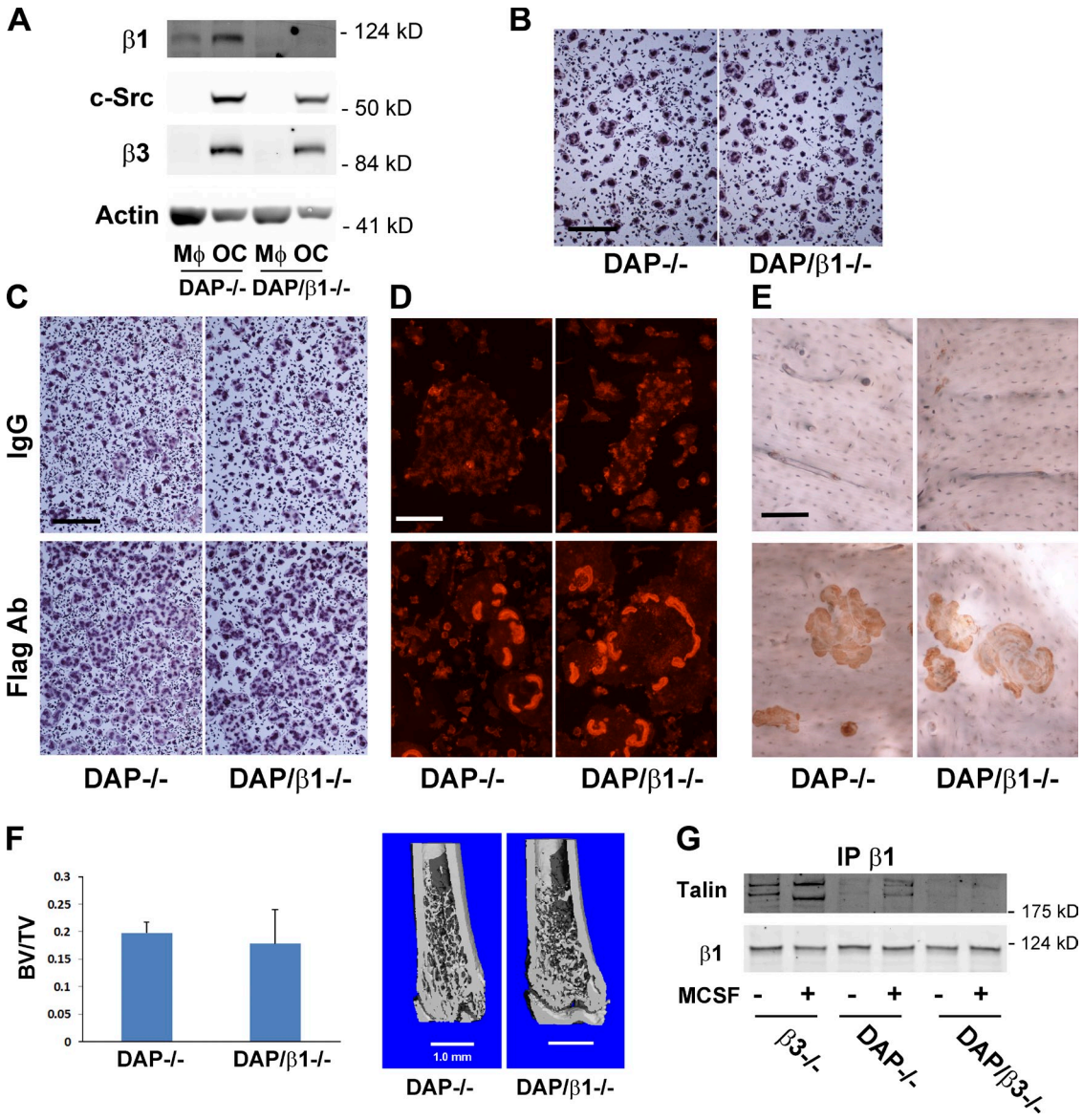

Figure 6. **Dap12/β3 deletion prevents compensatory integrin activation.** (A) $\beta1^{fl/fl}$ mice, mated to those lacking Dap12, were crossed to mice expressing LysMCre, yielding animals with myeloid lineage deletion of the β1 integrin and global absence of Dap12 (DAP/$\beta1^{-/-}$). BMMs were exposed to RANKL and M-CSF and the osteoclast differentiation proteins, β3 and c-Src, immunoblotted after 3 d. $Dap12^{-/-}/\beta1^{fl/fl}$ cells ($Dap^{-/-}$) serve as control. (B) DAP/$\beta1^{-/-}$ and $DAP^{-/-}$ BMMs, exposed to M-CSF and RANKL for 5 d, were stained for TRAP activity. Bar, 500 µm. (C) DAP/$\beta1^{-/-}$ and $DAP^{-/-}$ BMMs were transduced with OSCAR-FLAG. The cells were plated on IgG or anti-FLAG Ab in the presence of M-CSF and RANKL. After 5 d, the cells were stained for TRAP activity. Bar, 500 µm. (D) DAP/$\beta1^{-/-}$ and $DAP^{-/-}$ BMMs were transduced with OSCAR-FLAG or vector. The cells were plated on bone in the presence of M-CSF and RANKL. After 5 d, the cells were stained with Alexa Fluor 543-phalloidin to visualize actin rings. Bar, 100 µm. (E) DAP/$\beta1^{-/-}$ and $DAP^{-/-}$ BMMs were transduced with OSCAR-FLAG or vector. The cells were plated on bone in the presence of M-CSF and RANKL. After 5 d, the cells were removed and resorption pits were visualized by peroxidase-conjugated wheat germ agglutinin/horse radish peroxidase staining. Bar, 100 µm. (F) DAP/$\beta1^{-/-}$ and $DAP^{-/-}$ mouse tibia were subjected to µCT analysis and BV/TV determined. (G) $\beta3^{-/-}$, $Dap12^{-/-}$, and DAP/$\beta1^{-/-}$ BMMs were treated with RANKL and M-CSF for 3 d. Cytokine/serum starved cells were exposed to M-CSF (+) or PBS (−) for 5′. β1 immunoprecipitates were immunoblotted for talin and β1.

integrin in osteoclasts, and thus we engineered mice lacking the β3 subunit (McHugh et al., 2000). In addition to compromised ability to bind matrix, osteoclasts generated from $\beta3^{-/-}$ BMMs do not optimally spread, suggesting cytoskeletal dysfunction. In fact, such dysfunction represents failure to activate a cytoskeleton-organizing signaling complex containing the integrin, c-Src, and Syk, ultimately leading to activation of the small GTPase Rac. Deletion of any component of this complex yields poorly spread osteoclasts. Whereas absence of c-Src, Syk, or Rac yields severe osteopetrosis, αvβ3-deficient mice exhibit no increase in bone mass until at least 4 mo of age (Soriano et al., 1991; McHugh et al., 2000; Zou et al., 2007; Croke et al., 2011).

Koga et al. (2004) and Mócsai et al. (2004) have documented that combined deletion of Dap12 and FcRγ causes severe osteopetrosis. The authors reasoned that Dap12 deficiency, but not that of FcRγ, inhibits osteoclast formation in vitro and concluded that Dap12 is the principal co-stimulatory molecule regulating the bone resorptive cell. Inconsistent with Dap12 mediating differentiation of the cell, Mócsai et al. (2004) noted that osteoclast maturation markers are normally expressed despite

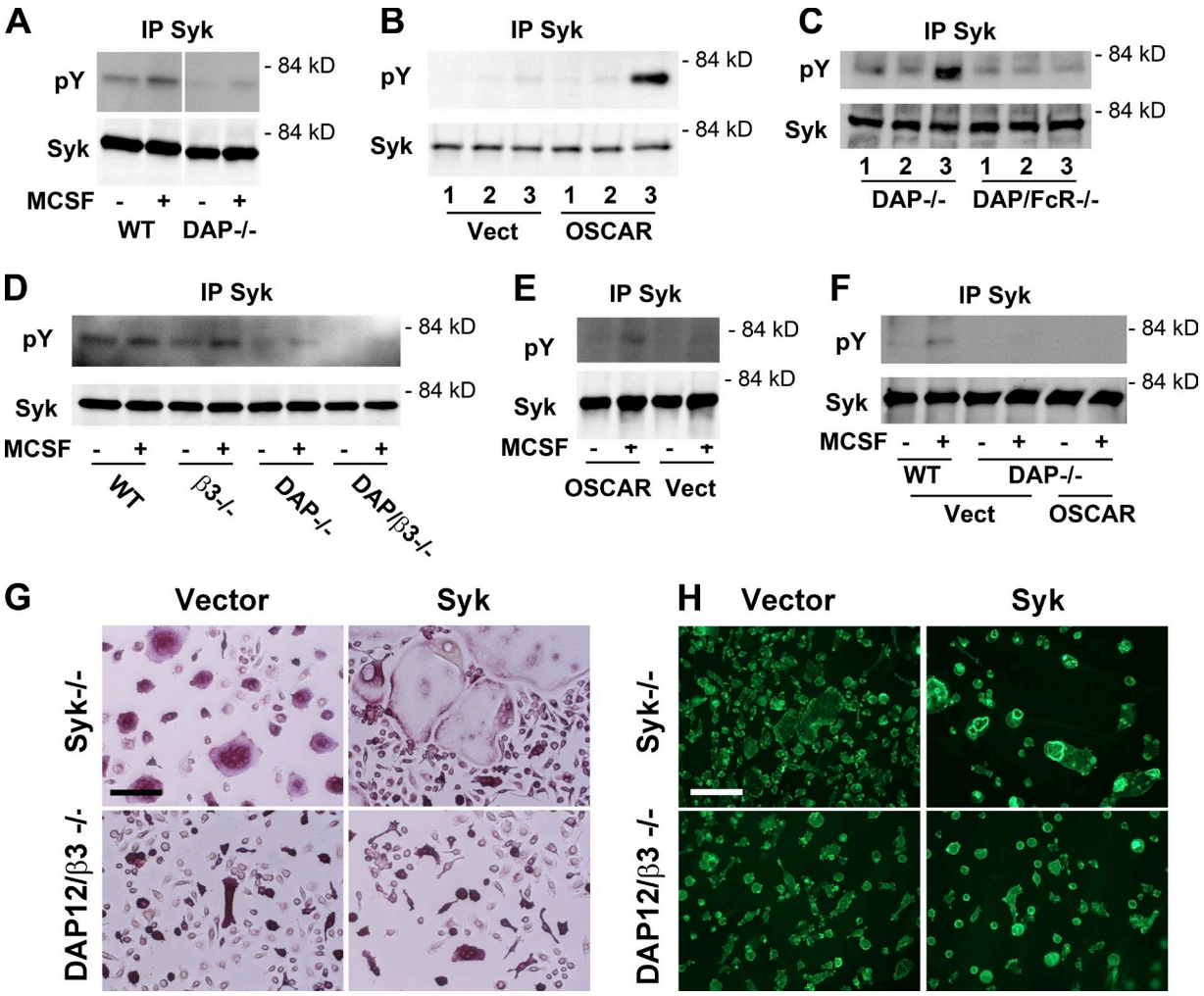

Figure 7. **Syk activation is disrupted in DAP/β3$^{-/-}$ osteoclasts.**. (A) WT and Dap12$^{-/-}$ BMMs were cultured on bone for 3 d in the presence of RANKL and M-CSF. Cytokine/serum starved cells were exposed to M-CSF or PBS for 30 min. Syk immunoprecipitates were immunoblotted with an antiphosphotyrosine mAb. (B) Dap12$^{-/-}$ BMMs, transduced with OSCAR-FLAG or vector were exposed to M-CSF and RANKL for 3 d. The cells were suspended and cytokine/serum starved, after which they were maintained in suspension (lane 1) or plated on vitronectin (lane 2) or vitronectin + anti-FLAG Ab (lane 3). Syk immunoprecipitates were immunoblotted with an anti-phosphotyrosine mAb. (C) Dap12$^{-/-}$ and Dap12$^{-/-}$/FcRγ$^{-/-}$ BMMs, transduced with OSCAR-FLAG were exposed to M-CSF and RANKL for 3 d. The cells were suspended and cytokine/serum starved, after which they were maintained in suspension (lane 1) or plated on vitronectin (lane 2) or vitronectin + anti-FLAG mAb (lane 3). Syk immunoprecipitates were immunoblotted with an antiphosphotyrosine mAb. (D) Dap12$^{-/-}$ and DAP/β3$^{-/-}$ BMMs, transduced with OSCAR-FLAG, were exposed to M-CSF and RANKL, on bone, for 3 d. The cells were cytokine/serum starved, after which they were exposed to M-CSF or PBS for 5 min. Syk immunoprecipitates were immunoblotted with an antiphosphotyrosine mAb. (E) Dap12$^{-/-}$ BMMs, transduced with OSCAR-FLAG or vector and plated on bone, were exposed to M-CSF and RANKL for 3 d. Cells were cytokine/serum starved after which they were exposed to M-CSF for 5 min. Syk immunoprecipitates were immunoblotted with an antiphosphotyrosine mAb. (F) Dap12$^{-/-}$ BMMs, transduced with OSCAR-FLAG or vector, were cultured on plastic in the absence of anti-FLAG mAb, for 3 d. Cytokine/serum starved cells were exposed to M-CSF or PBS for 5 min, after which Syk immunoprecipitates were immunoblotted with an anti-phosphotyrosine mAb. Vector-transduced WT cells serve as control. (G and H) Syk$^{-/-}$ and DAP/β3$^{-/-}$ BMMs transduced with Syk or vector were cultured in the presence of M-CSF and RANKL on plastic (left) or (right) bone. After 5 d, plastic-residing cells were stained for TRAP activity and those on bone were stained with Alexa Fluor 488-phalloidin to visualize actin rings. Bar, 100 µm.

absence of the ITAM protein. Subsequent studies establish that the principal effect of Dap12 deficiency, in osteoclasts, is not arrested differentiation but cytoskeletal and resorptive dysfunction whether or not FcRγ is co-deleted (Zou et al., 2007, 2010)

Perhaps the most surprising feature of these two studies is the discrepancy between the in vitro appearance of Dap12$^{-/-}$ osteoclasts and lack of an impressive bone phenotype. Using co-cultures of mutant osteoclast linage cells and WT osteoblasts, both groups proposed that the absence of osteopetrosis in Dap12$^{-/-}$ mice reflects compensation by FcRγ. These experiments also raised the likelihood of an osteoblast-produced ligand recognizing FcRγ co-receptors such as OSCAR or PIR-A.

This study addresses the unresolved issue regarding the means by which FcRγ compensates for the absence of Dap12 in regulating osteoclastic bone resorption. We find that combined deletion of Dap12 and β3 yields severe osteopetrosis whereas absence of either of the two genes, alone, has minimal skeletal impact. This observation is unexpected in light of the linear signaling relationship of Dap12 and β3 and establishes the integrin is necessary for FcRγ to exert its compensatory effect. Like individual deletion of either the ITAM protein or integrin, their combined absence does not affect expression of osteoclast differentiation markers but causes substantially more severe cytoskeletal abnormalities. Our challenge was to determine the

molecular mechanism whereby αvβ3 mediates the salutary properties of FcRγ on Dap12$^{-/-}$ osteoclasts.

We documented that Dap12 exerts it cytoskeletal effects, in osteoclasts, by processes involving αvβ3 and M-CSF (Zou et al., 2007, 2008). This event entails activation of Rap1 which promotes talin association with β integrin cytoplasmic domains (Zou et al., 2013). The complex transits the integrin to its high affinity, ligand-binding state, thus inducing its cytoskeleton-organizing effectors. This observation is in keeping with evidence that other β integrins, particularly β1 which recognizes Syk, may compensate, in some circumstances, for absence of αvβ3 (Kamiguti et al., 2000). Although not yet confirmed in vivo, multiple integrin deletion in vitro yields a more severe cytoskeletal phenotype than absence of only one subunit (Schmidt et al., 2011).

Compensation of β3 deficiency, by β1, does not occur with co-deletion of Dap12. This observation also explains the mild skeletal effects of β3 deficiency compared with the robust osteopetrosis attending absence of talin, Rap1, or kindlin3 each of which globally targets β integrins. Failure of M-CSF to promote talin association with the β1 subunit in DAP/β3$^{-/-}$ cells, while it does so in those lacking a single gene, provides the key mechanistic insight into the severe osteopetrosis of DAP/β3$^{-/-}$ mice and why αvβ3 is required for FcRγ-mediated rescue of Dap12$^{-/-}$ osteoclasts. Suppression of β1/talin association by Dap12/β3 deletion is, however, surprising in light of evidence that β3 exerts a transdominant effect on β1 activation (Das et al., 2014). This transdominant effect is consistent with the robust interaction of talin and β1 in M-CSF–stimulated β3$^{-/-}$ osteoclasts (Zou et al., 2013). Thus, in the presence of Dap12, β3 deletion activates other integrins whereas in the absence of Dap12, β3 deficiency is suppressive. We believe these data provide the first example of deletion of a specific integrin activating or suppressing another, depending upon circumstance (Kamiguti et al., 2000). Although failure to activate β1 is likely central to the DAP/β3$^{-/-}$ skeletal phenotype, DAP/β1$^{-/-}$ mice and osteoclasts are indistinguishable from those lacking only Dap12. The essential partnership with FcRγ, in rescue of Dap12 deficiency is, therefore, likely unique to αvβ3.

Having noted that absence of αvβ3 and Dap12 obviates inside-out stimulation of a compensatory integrin, we turned to its effect on cytoskeletal signaling. We focused on Syk, as its activation is essential to osteoclast cytoskeletal organization, regardless of the inductive event. Furthermore, Syk has an established relationship with αvβ3 and ITAM proteins in the bone resorptive cell (Zou et al., 2007, 2008). Importantly, Dap12-induced signaling, in osteoclasts, is universally mediated by Syk, deletion of which also does not impair differentiation of these cells but disrupts their cytoskeleton (Zou et al., 2007). Upon integrin occupancy, liganded Dap12 is recruited to the β3 cytoplasmic domain, where it undergoes c-Src–mediated phosphorylation of its ITAM tyrosines which, in turn, recruit Syk (Zou et al., 2007). Subsequent phosphorylation of Syk activates a canonical, Rac-containing, cytoskeleton-organizing complex. A similar Syk-dependent pathway is activated by M-CSF via talin association with β3 or β1 subunits, thereby promoting mutual compensation by the integrins (Zou et al., 2013). Thus, an integrin in addition to αvβ3, also links M-CSF to Dap12/Syk-mediated cytoskeletal organization (Zou et al., 2008). Consistent with OSCAR ligand being a collagen peptide, M-CSF phosphorylates Syk, albeit modestly, in Dap12$^{-/-}$ osteoclasts cultured on bone, a phenomenon accentuated by enhancing OSCAR expression. Although the reason why FcRγ-mediated Syk phosphorylation is not optimized with physiological expression of OSCAR is unknown, it may represent competition by inhibitory receptors, such as PIR-B and FcγRIIβ, expressed by osteoclasts (Koga et al., 2004).

M-CSF also phosphorylates Syk in the absence of Dap12, but fails to do so in DAP/β3$^{-/-}$ osteoclasts. It appears, therefore, that whereas other integrins may partially compensate for lack of β3 in the presence of only Dap12 signaling, such is not the case in the context of FcRγ. This posture is in keeping with the fact that combined deletion of FcRγ and β3 yields osteoclasts indistinguishable from those lacking only the integrin and helps explain the dramatic skeletal phenotype of DAP/β3$^{-/-}$ mice.

These studies establish that the machinery compensating for absence of Dap12 or αvβ3 is ineffective when both are deleted and suggest the following model (Fig. 8). In WT osteoclasts Dap12 binds to liganded, high affinity αvβ3 to induce cytoskeletal organization. In the absence of Dap12, FcRγ substitutes by associating with αvβ3. When αvβ3 is lacking, other activated β integrins, such as those containing β1, effectively compensate. In contrast, normalization of osteoclasts lacking both Dap12 and αvβ3, by FcRγ, is not possible as activation of compensatory integrins is arrested.

Recent evidence indicates that arrest of osteoclast function is a more effective means of inhibiting bone loss than is diminution of cell number (Williams et al., 2013). The osteoclast cytoskeleton presents as a candidate therapeutic target in this regard, thus the mechanism by which the osteoclast organizes its cytoskeleton is important. In fact, blockade of αvβ3 has bone-sparing effects in osteoporotic women (Murphy et al., 2005). The present study underscores the unique and central role the integrin plays in osteoclast function and provides insights into how it does so in association with Dap12 and FcRγ.

Materials and methods

Mice

β3$^{-/-}$ mice were generated by using a targeting construct in which a 1.2-kb genomic fragment (including 300 bp of the promoter, the transcriptional start site, exon I, intron I, and exon II) was replaced by a phosphoglycerokinase promoter-neomycin resistance gene cassette (McHugh et al., 2000). Dap12$^{-/-}$ mice were provided by T. Takai (Tohoku University, Sendai, Japan), and were generated by standard gene-targeting methods that resulted in the deletion of a putative promoter and exons 1–3 of Dap12 (Kaifu et al., 2003). Dap12$^{-/-}$/β3$^{-/-}$ mice were generated by crossing between Dap12$^{-/-}$/β3$^{+/-}$males and females obtained by mating of Dap12$^{-/-}$ mice with β3$^{-/-}$ mice. β1$^{fl/fl}$ mice and Lys M-Cre mice were obtained from The Jackson Laboratory. FcRγ$^{-/-}$ mice, generated by a neomycin selection cassette, were inserted into exon2 creating a stop codon downstream of the integration site (Takai et al., 1994). Dap12$^{-/-}$/FcRγ$^{-/-}$, generated by cross mating of DAP12$^{-/-}$ mice with FcRγ$^{-/-}$ mice, were provided by M. Colonna (Washington University School of Medicine, St. Louis, MO). All mice were housed in the animal care unit of Washington University School of Medicine, where they were maintained according to guidelines of the Association for Assessment and Accreditation of Laboratory Animal Care. All animal experimentation was approved by the Animal Studies Committee of Washington University School of Medicine.

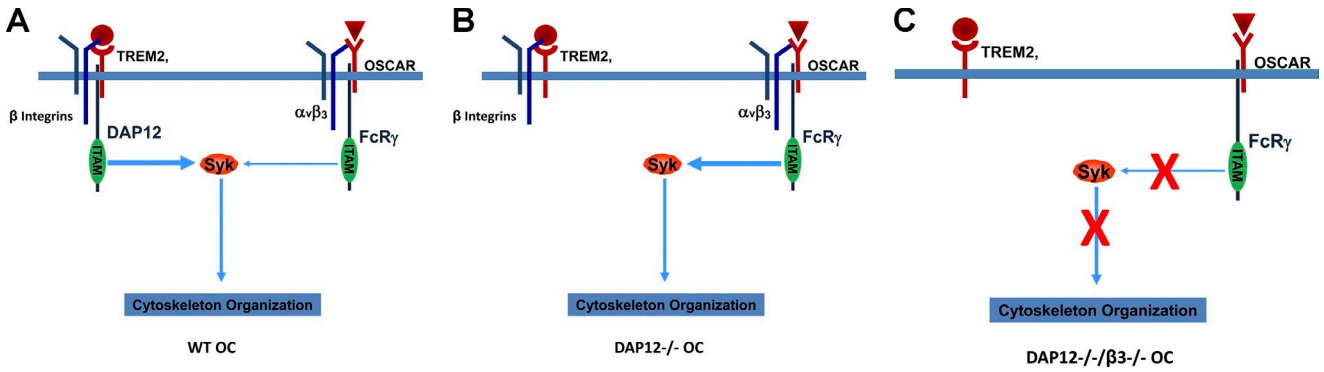

Figure 8. **Proposed model of OSCAR-FcRγ regulation by β3 integrin in osteoclasts.** (A) In WT osteoclasts the dominant mechanism of Syk activation and cytoskeletal organization is via TREM2-stimulated Dap12 complexed with β3 and β1 integrins. In this circumstance, OSCAR-induced FcRγ, interacting exclusively with αvβ3 makes a minimal, nonessential contribution. (B) In the absence of Dap12, Syk is activated exclusively by OSCAR-associated FcRγ in an αvβ3-dependent manner. (C) FcRγ is incapable of activating Syk without αvβ3, and thus cannot compensate for absence of Dap12, resulting in cytoskeletal disorganization.

Reagents

Recombinant murine M-CSF was obtained from R&D Systems. Glutathione-*S*-transferase (GST)-RANKL was expressed in our laboratory. The GST-RANKL vector was constructed by PCR cloning a SalI/NotI fragment corresponding to amino acids 158–316 of murine RANKL from osteoblast cDNA (forward primer, 5′-ATGTGGCCCGTCGACGCAAGCCTGAGGCCCAGCC-3′; reverse primer, 5′-AAACATCTAGGGCGGCCGCGCTAATG-3′) and cloning into pGEX-4T-1 (GE Healthcare). Both strands were sequenced. High-expressing BL21 (Stratagene) cells were lysed under nondenaturing conditions and GST-RANKL was purified over a glutathione-Sepharose column followed by ion exchange chromatography (Lam et al., 2000). The sources of antibodies were as follows: rabbit anti-integrin β3 (Cell Signaling Technology); mouse antiphosphotyrosine (4G10), rabbit anti-FcRγ from Millipore; mouse anti-NFATc1 and rabbit anti-Syk (N19; Santa Cruz Biotechnology, Inc.); mouse anti-Flag Ab, rabbit anti-Flag Ab, mouse anti-Talin Ab, and mouse anti-actin Ab (Sigma-Aldrich); mouse anti-HA Ab (Covance); goat anti-OSCAR Ab (R&D Systems); rabbit anti-β1 Ab (Abcam). All other chemicals were obtained from Sigma-Aldrich.

Macrophage isolation and osteoclast culture

Marrow was extracted from femora and tibiae of 4–8-wk-old mice with α-MEM and cultured in α-MEM containing 10% inactivated fetal bovine serum, 100 IU/ml penicillin, and 100 µg/ml streptomycin (α-10 medium) with 1:10 CMG condition media on Petri-plastic dishes. Cells were incubated at 37°C in 6% CO_2 for 3 d, and then washed with PBS and lifted with 1× trypsin/EDTA (Invitrogen) in PBS. A total of 5×10^3 cells were cultured in 200 µl α-MEM containing 10% heat-inactivated FBS with GST-RANKL and 30 ng/ml of mouse recombinant M-CSF in 96-well tissue culture plates, some containing sterile bone slices. For some experiments, cell culture plates were coated with 10 µg/ml anti-Flag Ab or IgG overnight at 4°C before cells were plated. Cells were fixed and stained for tartrate-resistant acid phosphatase (TRAP) activity after 6 d in culture, using a commercial kit (387-A; Sigma-Aldrich).

Calvarial osteoblast isolation and co-culture

Primary osteoblasts were extracted from 3–5-d-old neonatal calvariae with collagenase. 1.2×10^4 osteoblasts and 3×10^4 macrophages were mixed and cultured in α-10 culture medium in 48-well plates with 1,25-dihydroxyvitamin D (10^{-8} M) for 7 d. The osteoblasts were lifted by collagenase, and the remaining cells were stained for TRAP activity.

Plasmids and retroviral transduction

Mouse full-length Dap12 with a FLAG tag was cloned into the BamH1 and Not1 sites of the pMX-puro vector. Wild-type human β3 construct were subcloned into the *Bam*HI and *Xho*I sites of a pMX retroviral vector. pMX OSCAR plasmid (OSCAR without signal sequence was cloned into a pMX retrovirus expression vector containing human CD8 signal sequence and FLAG sequence) was provided by H. Arase (Osaka University, Osaka, Japan; Ishikawa et al., 2004). All genes in the pMX constructs were under CMV (Cytomegalovirus) promoter. cDNA was transfected transiently into Plat-E packaging cells using FuGENE 6 Transfection Reagent (Roche). Virus was collected 48 h after transfection. Macrophages were infected with virus for 24 h in the presence of 100 ng/ml M-CSF and 4 µg/ml polybrene (Sigma-Aldrich). Cells were selected in the presence of M-CSF and 1 µg/ml blasticidin (EMD Millipore) for 3 d before use as osteoclast precursors.

Actin ring and bone resorptive pit visualization

For actin ring staining, cells were cultured on bovine bone slices in the presence of M-CSF and RANKL for 6 d, after which cells were fixed in 4% paraformaldehyde, permeabilized in 0.1% Triton X-100, rinsed in PBS, and immunostained with Alexa Fluor 488-phalloidin (Molecular Probes). To quantitate resorption lacunae, cells were removed from bone slices with mechanical agitation. Bone slices were incubated with peroxidase-conjugated wheat germ agglutinin (WGA; Sigma-Aldrich) for 1 h and stained with 3,3′-diaminobenzidine (Sigma-Aldrich).

Western blot analysis and immunoprecipitation

Cultured cells were washed twice with ice-cold PBS and lysed in radioimmune precipitation assay (RIPA) buffer containing 20 mm Tris-HCl, pH 7.5, 150 mm NaCl, 1 mm EDTA, 1 mm EGTA, 1% Triton X-100, 2.5 mm sodium pyrophosphate, 1 mm β-glycerophosphate, 1 mm Na_3VO_4, 1 mm NaF, and 1× protease inhibitor mixture (Roche). Total cell lysates were prepared by homogenizing tissue in TNE lysis buffer consisting of 1% Triton X-100, 150 mM NaCl, 50 mM Tris, pH 7.4, and 2 mM EDTA supplemented with protease and phosphatase inhibitors. After incubation on ice for 10 min, cell lysates were clarified by centrifugation at 15,000 rpm for 10 min. 40 µg of total lysates were subjected to 8–12% sodium dodecyl sulfate PAGE and transferred onto PVDF membranes. Filters were blocked in 0.1% casein in PBS for 1 h and incubated with primary antibodies at 4°C overnight, followed by probing with either fluorescence-labeled secondary antibodies (Jackson ImmunoResearch Laboratories) or HRP-labeled secondary antibodies (Santa Cruz Biotechnology, Inc.). Proteins were detected with the Odyssey Infrared Imaging System (LI-COR Biosciences) or SuperSignal ECL solution (Thermo Fisher Scientific). For immunoprecipitation, 1 mg of protein was incubated with Ab at 4°C overnight with rotation. Protein A/G agarose (Santa Cruz Biotechnology, Inc.) was then added and incubated with rotation for 3 h at 4°C. Immunoprecipitates were washed three times in lysis buffer and the beads were boiled in 2× SDS sample buffer for 5 min. After centrifugation, proteins were separated by 8% SDS polyacrylamide gels.

Proliferation assay

Macrophages (plated in 96-well dishes at a density of 5,000 cells/well) were maintained for 3 d in α-10 medium with 20 ng/ml M-CSF and 100 ng/ml RANKL and labeled with BrdU for the last 3 h of culture. BrdU incorporation was determined using the Biotrak ELISA system (GE Healthcare).

Apoptosis assay

Macrophages (plated in 96-well dishes) were cultured with 20 ng/ml M-CSF and 100 ng/ml RANKL for 3 d. Cells were deprived of M-CSF for 5 h. Cell death was analyzed in quadruplicate using cell death detection ELISAPLUS kit (Roche), which detects cytoplasmic histone-associated DNA fragmentation.

Serum biomarkers

Blood was collected under anesthesia. Serum CTx concentration was determined with the RatLaps ELISA kit (Nordic Bioscience Diagnostics AS).

Serum osteocalcin was determined with the Mouse Osteocalcin EIA kit (Biomedical Technologies Inc.).

Microcomputed tomography (μCT)

The trabecular volume in the distal femoral metaphysis or proximal tibia was measured using a Scanco μCT40 scanner (Scanco Medical AG). A threshold of 220 was used for evaluation of all scans. 40–100 slices were analyzed, starting with the first slice in which condyles and primary spongiosa were no longer visible.

Histology and histomorphometry

The mice tibiae were fixed with 10% neutral buffered formalin, followed by decalcification in 14% EDTA for 10 d, paraffin embedding, and TRAP staining. Osteoclastic and osteoblastic perimeters were measured and analyzed using BioQuant OsteoII (BioQuant Image Analysis Corporation) in a blinded fashion.

Statistics

Statistical significance was determined using Student's *t* test or ANOVA. *, $P < 0.05$; **, $P < 0.01$; ***, $P < 0.001$ in all experiments.

Image acquisition and manipulation

Images from Fig. 1 E, Fig. 2 (A–C, F, and K), Fig. 3 (A and B), Fig. 4 (A, B, and D), Fig. 6 (B–E), Fig. 7 (G and H), and Fig. S1 were acquired using a microscope (Eclipse E400; Nikon) with plan Fluor lenses at room temperature. No imaging media were used except for Fig. 2 F. Zimmerson oil (Thermo Fisher Scientific) served as the imaging medium in Fig. 2 F. Fluorochrome Alexa Fluor 543 was used in Fig. 2 B, Fig. 4 B, and Fig. 6 D. Fluorochrome FITC was used in Fig. 7 H and Fig. S1. Photographs were taken with a camera (Nikon Digital Sight DS-Fi1) and displayed with NIS-Elements software (F3.0) in all circumstances except Fig. 1 A. The images were organized in Photoshop (version 7.0.1; Adobe). Fig. 1 A was acquired with a digital camera (Powershot A75; Canon) and organized in Photoshop.

Online supplemental material

Fig. S1 shows that in the presence of β3 integrin, OSCAR activation increases DAP/β3$^{-/-}$ osteoclast spreading and rescues DAP/β3$^{-/-}$ osteoclast function on bone. Online supplemental material is available at http://www.jcb.org/cgi/content/full/jcb.201410123/DC1.

The authors wish to thank Jean Chappel for technical assistance and Marco Colonna for review of the manuscript.

This work was supported by National Institutes of Health grants 5R01AR03278828, 5R01AR05703705, and 5R37AR04652315 (SLT) and P30 AR057235.

The authors declare no competing financial interests.

Submitted: 29 October 2014
Accepted: 1 December 2014

References

Barrow, A.D., N. Raynal, T.L. Andersen, D.A. Slatter, D. Bihan, N. Pugh, M. Cella, T. Kim, J. Rho, T. Negishi-Koga, et al. 2011. OSCAR is a collagen receptor that costimulates osteoclastogenesis in DAP12-deficient humans and mice. *J. Clin. Invest.* 121:3505–3516. http://dx.doi.org/10.1172/JCI45913

Calderwood, D.A., V. Tai, G. Di Paolo, P. De Camilli, and M.H. Ginsberg. 2004. Competition for talin results in trans-dominant inhibition of integrin activation. *J. Biol. Chem.* 279:28889–28895. http://dx.doi.org/10.1074/jbc.M402161200

Croke, M., F.P. Ross, M. Korhonen, D.A. Williams, W. Zou, and S.L. Teitelbaum. 2011. Rac deletion in osteoclasts causes severe osteopetrosis. *J. Cell Sci.* 124:3811–3821. http://dx.doi.org/10.1242/jcs.086280

Das, M., S. Subbayya Ithychanda, J. Qin, and E.F. Plow. 2014. Mechanisms of talin-dependent integrin signaling and crosstalk. *Biochim. Biophys. Acta*. 1838:579–588.

Faccio, R., D.V. Novack, A. Zallone, F.P. Ross, and S.L. Teitelbaum. 2003a. Dynamic changes in the osteoclast cytoskeleton in response to growth factors and cell attachment are controlled by beta3 integrin. *J. Cell Biol.* 162:499–509. http://dx.doi.org/10.1083/jcb.200212082

Faccio, R., W. Zou, G. Colaianni, S.L. Teitelbaum, and F.P. Ross. 2003b. High dose M-CSF partially rescues the Dap12-/- osteoclast phenotype. *J. Cell. Biochem.* 90:871–883. http://dx.doi.org/10.1002/jcb.10694

Helfrich, M.H., S.A. Nesbitt, P.T. Lakkakorpi, M.J. Barnes, S.C. Bodary, G. Shankar, W.T. Mason, D.L. Mendrick, H.K. Väänänen, and M.A. Horton. 1996. Beta 1 integrins and osteoclast function: involvement in collagen recognition and bone resorption. *Bone*. 19:317–328. http://dx.doi.org/10.1016/S8756-3282(96)00223-2

Humphrey, M.B., L.L. Lanier, and M.C. Nakamura. 2005. Role of ITAM-containing adapter proteins and their receptors in the immune system and bone. *Immunol. Rev.* 208:50–65. http://dx.doi.org/10.1111/j.0105-2896.2005.00325.x

Ishikawa, S., N. Arase, T. Suenaga, Y. Saita, M. Noda, T. Kuriyama, H. Arase, and T. Saito. 2004. Involvement of FcRgamma in signal transduction of osteoclast-associated receptor (OSCAR). *Int. Immunol.* 16:1019–1025. http://dx.doi.org/10.1093/intimm/dxh103

Kaifu, T., J. Nakahara, M. Inui, K. Mishima, T. Momiyama, M. Kaji, A. Sugahara, H. Koito, A. Ujike-Asai, A. Nakamura, et al. 2003. Osteopetrosis and thalamic hypomyelinosis with synaptic degeneration in DAP12-deficient mice. *J. Clin. Invest.* 111:323–332. http://dx.doi.org/10.1172/JCI16923

Kamiguti, A.S., R.D. Theakston, S.P. Watson, C. Bon, G.D. Laing, and M. Zuzel. 2000. Distinct contributions of glycoprotein VI and alpha(2)beta(1) integrin to the induction of platelet protein tyrosine phosphorylation and aggregation. *Arch. Biochem. Biophys.* 374:356–362. http://dx.doi.org/10.1006/abbi.1999.1627

Koga, T., M. Inui, K. Inoue, S. Kim, A. Suematsu, E. Kobayashi, T. Iwata, H. Ohnishi, T. Matozaki, T. Kodama, et al. 2004. Costimulatory signals mediated by the ITAM motif cooperate with RANKL for bone homeostasis. *Nature*. 428:758–763. http://dx.doi.org/10.1038/nature02444

Lam, J., S. Takeshita, J.E. Barker, O. Kanagawa, F.P. Ross, and S.L. Teitelbaum. 2000. TNF-alpha induces osteoclastogenesis by direct stimulation of macrophages exposed to permissive levels of RANK ligand. *J. Clin. Invest.* 106:1481–1488. http://dx.doi.org/10.1172/JCI11176

McHugh, K.P., K. Hodivala-Dilke, M.H. Zheng, N. Namba, J. Lam, D. Novack, X. Feng, F.P. Ross, R.O. Hynes, and S.L. Teitelbaum. 2000. Mice lacking β3 integrins are osteosclerotic because of dysfunctional osteoclasts. *J. Clin. Invest.* 105:433–440. http://dx.doi.org/10.1172/JCI8905

Mócsai, A., M.B. Humphrey, J.A. Van Ziffle, Y. Hu, A. Burghardt, S.C. Spusta, S. Majumdar, L.L. Lanier, C.A. Lowell, and M.C. Nakamura. 2004. The immunomodulatory adapter proteins DAP12 and Fc receptor gamma-chain (FcRgamma) regulate development of functional osteoclasts through the Syk tyrosine kinase. *Proc. Natl. Acad. Sci. USA*. 101:6158–6163. http://dx.doi.org/10.1073/pnas.0401602101

Murphy, M.G., K. Cerchio, S.A. Stoch, K. Gottesdiener, M. Wu, and R. Recker. L-000845704 Study Group. 2005. Effect of L-000845704, an alphaV-beta3 integrin antagonist, on markers of bone turnover and bone mineral density in postmenopausal osteoporotic women. *J. Clin. Endocrinol. Metab.* 90:2022–2028. http://dx.doi.org/10.1210/jc.2004-2126

Novack, D.V., and S.L. Teitelbaum. 2008. The osteoclast: friend or foe? *Annu. Rev. Pathol.* 3:457–484. http://dx.doi.org/10.1146/annurev.pathmechdis.3.121806.151431

Schmidt, S., I. Nakchbandi, R. Ruppert, N. Kawelke, M.W. Hess, K. Pfaller, P. Jurdic, R. Fässler, and M. Moser. 2011. Kindlin-3-mediated signaling from multiple integrin classes is required for osteoclast-mediated bone resorption. *J. Cell Biol.* 192:883–897. http://dx.doi.org/10.1083/jcb.201007141

Soriano, P., C. Montgomery, R. Geske, and A. Bradley. 1991. Targeted disruption of the c-src proto-oncogene leads to osteopetrosis in mice. *Cell*. 64:693–702. http://dx.doi.org/10.1016/0092-8674(91)90499-O

Takai, T., M. Li, D. Sylvestre, R. Clynes, and J.V. Ravetch. 1994. FcR gamma chain deletion results in pleiotrophic effector cell defects. *Cell*. 76:519–529. http://dx.doi.org/10.1016/0092-8674(94)90115-5

Tolar, J., S.L. Teitelbaum, and P.J. Orchard. 2004. Osteopetrosis. *N. Engl. J. Med.* 351:2839–2849. http://dx.doi.org/10.1056/NEJMra040952

Williams, D.S., P.J. McCracken, M. Purcell, M. Pickarski, P.D. Mathers, A.T. Savitz, J. Szumiloski, R.Y. Jayakar, S. Somayajula, S. Krause, et al. 2013. Effect of odanacatib on bone turnover markers, bone density and geometry of the spine and hip of ovariectomized monkeys: a head-to-head comparison with alendronate. *Bone*. 56:489–496. http://dx.doi.org/10.1016/j.bone.2013.06.008

Zou, W., H. Kitaura, J. Reeve, F. Long, V.L.J. Tybulewicz, S.J. Shattil, M.H. Ginsberg, F.P. Ross, and S.L. Teitelbaum. 2007. Syk, c-Src, the alphavbeta3 integrin, and ITAM immunoreceptors, in concert, regulate osteoclastic bone resorption. *J. Cell Biol.* 176:877–888. http://dx.doi.org/10.1083/jcb.200611083

Zou, W., J.L. Reeve, Y. Liu, S.L. Teitelbaum, and F.P. Ross. 2008. DAP12 couples c-Fms activation to the osteoclast cytoskeleton by recruitment of Syk. *Mol. Cell*. 31:422–431. http://dx.doi.org/10.1016/j.molcel.2008.06.023

Zou, W., T. Zhu, C.S. Craft, T.J. Broekelmann, R.P. Mecham, and S.L. Teitelbaum. 2010. Cytoskeletal dysfunction dominates in DAP12-deficient osteoclasts. *J. Cell Sci.* 123:2955–2963. http://dx.doi.org/10.1242/jcs.069872

Zou, W., T. Izawa, T. Zhu, J. Chappel, K. Otero, S.J. Monkley, D.R. Critchley, B.G. Petrich, A. Morozov, M.H. Ginsberg, and S.L. Teitelbaum. 2013. Talin1 and Rap1 are critical for osteoclast function. *Mol. Cell. Biol.* 33:830–844. http://dx.doi.org/10.1128/MCB.00790-12